

Research

Imbibition Assisted Oil RecoveryOrkhan H. Pashayev*, Erwinsyah Putra^{*§}, Dewi T. Hidayati*, David S. Schechter*

Address: Petroleum Engineering Department, Texas A&M University, Texas, USA

<http://pumpjack.tamu.edu/Faculty&Staff/faculty/schechter/baervan/homepage.html>

*These authors contributed equally to this work

§Corresponding author

Email: Orkhan H. Pashayev- pashayev@yahoo.com; Erwinsyah Putra[§] - putra@tamu.edu; Dewi T. Hidayati - dewi@tamu.edu; David S. Schechter - schech@spindletop.tamu.edu

*These authors contributed equally to this work

§Corresponding author

Published: 09 August 2005

Received: 30 June 2005

E-Journal of Reservoir Engineering 2005, ISSN: 1715-4677.

Accepted: 09 Aug 2005

This article is available from: <http://www.petroleumjournals.com/>

© 2005 Pashayev et al; licensee Petroleum Journals Online.

This is an Open Access article distributed under the terms of the Creative Commons Attribution License (<http://creativecommons.org/licenses/by-nd/2.0/>), which permits unrestricted use for non-commercial purposes, distribution, and reproduction in any medium, provided the original work is properly cited.**Abstract****Background**

Imbibition describes the rate of mass transfer between the rock and the fractures. Therefore, understanding the imbibition process and the key parameters that control the imbibition process is crucial. Capillary imbibition experiments usually take a long time, especially when we need to vary some parameters to investigate their effects. Therefore, this research presented the numerical studies with the matrix block surrounded by the wetting phase for better understanding the characteristic of spontaneous imbibition, and also evaluated dimensionless time for validating the scheme of upscaling laboratory imbibition experiments to field dimensions.

Results

Numerous parametric studies have been performed within the scope of this research. The results were analyzed in detail to investigate oil recovery during spontaneous imbibition with different types of boundary conditions. The results of these studies have been upscaled to the field dimensions. The validity of the new definition of characteristic length used in the modified scaling group has been evaluated. The new scaling group used to correlate simulation results has been compared to the early upscaling technique.

Conclusions

The research revealed the individual effects of various parameters on imbibition oil recovery. Also, the study showed that the characteristic length and the new scaling technique significantly improved upscaling correlations.

Background

It has been estimated that 30% of the oil production of the world comes from naturally fractured reservoirs. Naturally fractured reservoirs are typically considered as a dual-porosity system, which is composed of two distinct media: the matrix and the fractures. The matrix has high porosity but low

permeability, and the fractures have very high permeability and low porosity. This combination means that most of oil and gas is stored in the matrix and the fractures system provides the main channel for fluid flow. A successful recovery process is the one that recovers hydrocarbon from the low-permeability high-porosity matrix. Because of the interactions between the matrix and the fracture, the

characteristics of the fluid flow in the naturally fractured reservoirs are quite different from those of conventional single-porosity reservoirs. Some of the tasks in the recent modeling studies of naturally fractured reservoirs include the following main steps: geological fracture characterization, hydraulic characterization of fractures, upscaling of fractured reservoir properties, and fractured reservoir simulation.

In the dual porosity model, the fluid flow between the matrix blocks and the surrounding fractures is characterized by the transfer functions. For the transfer functions, it is a prerequisite that they accurately describe the multiphase flow between the matrix and the surrounding fractures. The expulsion of oil from the matrix blocks to the surrounding fractures by capillary imbibition of water is one of the most important oil recovery mechanisms in naturally fractured reservoirs with the low-permeability rock matrix, since in such reservoirs the conventional methods of production, such as building a pressure difference across matrix blocks, fail because of the high-permeability fracture network.

Water imbibition is a primary component of fluid transfer from the matrix to the fracture. Two approaches are generally used to describe the flow from the matrix blocks to the fractures and within the matrix blocks themselves: numerical and analytical. Numerical modeling requires intensive computer programming. The relations among the model parameters are often obscured inside of complex nonlinear expressions. Analytical solutions may provide more necessary physical insights about the effect of the model parameters and help better understand imbibition mechanisms to predict and optimize oil recovery. In turn, this can help to refine existing numerical models and/or develop better models in the future.

The importance of capillary imbibition was identified by the early investigators. Brownscombe and Dyes suggested that imbibition flooding could contribute to oil production from the Spraberry trend of West Texas.¹ This study established that for applying successful imbibition flood, the rock has to be preferentially water-wet and the rock surface exposed to imbibition should be as large as possible. Kleppe and Morse² suggested a two-dimensional numerical model which was able to simulate flow of water and oil in the matrix block as well as in the fractures. The fractures were represented by horizontal and vertical flow channels surrounding the matrix blocks.

The published studies have been concerned with different conditions under which water imbibition

occurs. Geometrical shape and size of the samples, boundary conditions, effects of gravity, type of fluids, and flowing conditions of the fluid surrounding the rock blocks are among the many factors that have been considered. Oil recovery by water imbibition displacement has concentrated on evaluating the relationship between time and oil production rate.

Motivation and Objectives

Different critical aspects of the capillary imbibition process have received a limited treatment in the petroleum literature. None of the recent papers devoted to capillary imbibition studies investigated the numerical scale-up of the process. Most authors checked the validity of their numerical models against data from the imbibition tests involving the same boundary conditions. Early scaling studies of spontaneous imbibition mostly focused on the shape factor, while there is no emphasis on endpoint mobilities. Large discrepancies among the scaled curves brought up the effect of sample heterogeneity, which is not well studied yet.

The objectives of the present study are to conduct numerical studies with the matrix block surrounded by the wetting phase for better understanding the characteristic of spontaneous imbibition, and also evaluate dimensionless time for validating the scheme of upscaling laboratory imbibition experiments to field dimensions. The purpose here is to isolate the individual effects of various parameters on imbibition recovery. This study addresses the importance of characterizing the imbibition mechanism for analysis of reservoir performance.

Methodology

Numerical modeling of the spontaneous imbibition experiment was performed using a two-phase black-oil commercial simulator (CMGTM). The experimental results from water static imbibition experiments have been acquired.³

Numerous parametric studies were performed and the results were analyzed in detail to investigate oil recovery during spontaneous imbibition with different types of boundary conditions. These studies included the effect of varying mobility ratio, different fracture spacing, different capillary pressure, different relative permeabilities, and varying permeability profiles along the core.

The results of these studies were upscaled to the field dimensions. The validity of the new definition of characteristic length used in the modified scaling group was evaluated based on our model. The new scaling group used to correlate simulation results was compared to early upscaling technique.

Available Data The spontaneous imbibition tests were performed using an imbibition apparatus shown in **Fig. 1**.³ The apparatus is a simple glass container equipped with a graduated glass cap. To perform an imbibition test, a core sample was immersed in the glass container filled with preheated brine. The container was then covered with a graduated cap. After filling the cap full with brine, the container was then stored in an air bath that had been set at constant temperature of 138 °F. Due to capillary imbibition action, oil was displaced from the core sample by the imbibing brine. The displaced oil accumulated in the graduated cap by gravity segregation. During the experiment, the volume of produced oil was recorded against time. The physical properties of the core sample and synthetic brine are listed in **Table 1**. **Fig. 2** presents the cumulative oil production from the core sample as a function of time. The portion of the oil recovery curve corresponding to the early times represents maximum rate of imbibition and the deviation of the oil recovery curve is caused by slowing down the imbibition rate. The imbibition rate slows down, as all the major channels of flow are already filled. Later, the curve completely bends over and the rate of imbibition is drastically reduced. At this stage, a very slow change in water saturation within time is observed in the core. The final water saturation in the core reached 55.32%.

Numerical Modeling

Discretization and Grid Sensitivity Analysis.

The core was completely surrounded by a wetting phase. Therefore, all faces of the core were at a constant water saturation of 1.0. All the rest of the core, prior to the experiment, was at constant initial water saturation, as was expressed by the initial conditions. Hence, the boundary conditions for this experiment were:

$$\begin{aligned} S_w(x, y, z, t) &= 1, x = 0 \\ S_w(x, y, z, t) &= 1, y = 0 \\ S_w(x, y, z, t) &= 1, z = 0 \\ S_w(x, y, z, t) &= 1, x = 1 \\ S_w(x, y, z, t) &= 1, y = 1 \\ S_w(x, y, z, t) &= 1, z = 1 \end{aligned} \quad (1)$$

To simulate the experiment numerically, the core was discretized into a grid model. An extra gridblock of very small dimensions was added at the top, bottom, and all over the sides of the core to account for the boundary condition. This gridblock was assigned a water saturation value of 1.0. To keep this value constant at all times, the pore volume of this gridblock was multiplied by a huge number.

Grid sensitivity analysis has been performed to determine an optimal grid size of the model, to accurately represent fluid flow and yet maintain relatively fast simulation run. To investigate the sensitivity to a grid size, the initial model has been refined from coarse into fine grid. **Table 2** shows five Cartesian grid sizes, which has been investigated in sensitivity analysis.

Decision on an optimal grid size has been made based on the analysis of oil recovery curves and computer CPU times. The comparisons of the results are shown in **Figs. 3** and **4**. **Fig. 3** represents oil recovery curves vs. time for five grid sizes. It can be seen that although oil recoveries for the grid sizes $7 \times 7 \times 7$ and $16 \times 16 \times 16$ are different, as we refine the grid size the difference becomes very little. Thus, the difference in oil recoveries between the case with $20 \times 20 \times 20$ grid size and the case with $20 \times 20 \times 25$ grid size is almost negligible.

Fig. 4 has been developed to demonstrate the effect of the grid size refinement on the total simulation time and also to help us determine the optimal number of gridblocks. Theoretically, the time for solving the pressure equation in gridblock simulation increases exponentially. At a certain number of gridblocks, the exponential increase becomes more obvious. Our own analysis determined that this point occurred at 8,000 gridblocks, which corresponds to the grid size of $20 \times 20 \times 20$. Therefore, based on the grid sensitivity analysis, it was decided to use the grid size of $20 \times 20 \times 20$. As shown in **Fig. 4**, it took around 90 seconds to simulate this case. Additional information of this model is presented in **Table 3**.

Matching Experimental Results. The primary objectives of matching were to improve and validate the reservoir simulation data. In general, the use of the initial simulation input data does not match the historical reservoir performance to a level that is acceptable for making an accurate future forecast. The final matched model is not unique. In other words, several different matched models may provide equally acceptable matches to past reservoir performance, but may yield significantly different future predictions. However, matching as much production data as available and adjusting only the least known reservoir data within the acceptable ranges should yield a better match.⁴⁴

In our case, the only available data we had was the cumulative oil production from the core sample as a function of time. This data was matched by trial and error estimates of relative permeability and capillary pressure. **Fig. 5** is a comparison of the observed oil recovery vs. the simulated oil recovery. A very poor match could be observed from this figure.

Relative Permeability and Capillary Pressure. Relative permeability was modeled using the power law correlations built in the commercial simulator CMG™. The values of end-point permeabilities were varied to obtain the best match. The capillary pressure was modeled by trial and error solution. **Table 4** shows the relative permeabilities and the capillary pressure values obtained for this match. The match of the recovery is shown in **Fig. 6**. The distance of the water imbibed into the core plug is demonstrated by the water saturation profile as shown in **Fig. 7**. As time increases, more water is imbibed into the core plug and, in turn, more oil is recovered.

Boundary Conditions. Once the model has been satisfactorily built, different types of boundary conditions have been studied. Oil recoveries by spontaneous imbibition model have been investigated for the following boundary conditions:

1. All Faces Open (AFO): The base case had "All Faces Open" type of boundary condition. This meant that all faces of the core were open to imbibition, i.e., a wetting phase imbibed into the core from all sides.
2. Two Ends Open (TEO): "Two Ends Open" type of boundary condition has been applied to the base case model. This type of imbibition model refers to the matrix block with only two faces at the top and bottom open to imbibition. The sides of the core were closed for a wetting phase to imbibe. The boundary conditions for this model were as follows:

$$\begin{aligned} S_w(x, y, z, t) &= 1, x = 0 \\ S_w(x, y, z, t) &= 1, y = 0 \end{aligned} \quad (2)$$

$$\begin{aligned} S_w(x, y, z, t) &= 1, x = L_x \\ S_w(x, y, z, t) &= 1, y = L_y \end{aligned}$$

3. Two Ends Closed (TEC): "Two Ends Closed" type of boundary condition refers to the imbibition model with two impermeable faces at the top and the bottom. For this type of imbibition, the flow occurs simultaneously through four faces of the matrix block. The boundary conditions for this type of the model were as follows:

$$\begin{aligned} S_w(x, y, z, t) &= 1, z = 0 \\ S_w(x, y, z, t) &= 1, z = L_z \end{aligned} \quad (3)$$

4. One End Open (OEO): "One End Open" type of boundary condition assumed that the imbibition

occurred only through one face. In our case a wetting phase imbibed through the bottom of the core. The boundary conditions for OEO type of the model were as follows:

$$\begin{aligned} S_w(x, y, z, t) &= 1, x = L_x \\ S_w(x, y, z, t) &= 1, y = L_y \end{aligned} \quad (4)$$

The schematic representation of Two Ends Open, Two Ends Closed, and One End Open types of boundary conditions is shown in **Fig. 8**. In all cases a wetting phase was in contact with the core at all times. To account for this effect, a water saturation value of 1.0 was assigned to a very small extra gridblock. The water saturation of this gridblock was kept constant at all times. To achieve constant water saturation, the pore volume of gridblock is multiplied by a big number.

Effect of Gravity. Although gravity has an effect on imbibition, it was neglected in current study. It was assumed that capillary forces are dominant and gravity forces are negligible. In order to do this, Bond number needs to be adjusted. Bond number is a measure of relative effect of gravity forces to that of capillary forces. The expression for Bond number is as follows:

$$B_o = \frac{g(\rho_1 - \rho_2)H^2}{s} \quad (5)$$

where g is gravitational acceleration, ρ_1 and ρ_2 are the densities of a wetting and a nonwetting phase accordingly, H is the height of the core, and s is surface tension. When $B_o \gg 1$, capillarity is negligible, if $B_o \ll 1$, then gravity is negligible.

Although the height of the core was very small, it was decided to reduce the effect of the gravity by making density difference equal to zero. The density of water has been changed from 1 g/cm³ to 0.8635 g/cm³ which was equal to the density of oil. This way the value of Bond number has been set to zero, which meant that the gravity effect is negligible. **Fig. 9** shows the effect of the gravity on oil recovery. From the figure it was observed that the gravity effect was not so prominent and neglecting it did not significantly affect the oil recovery.

Rates of Imbibition. The comparative study of spontaneous imbibition rates of water for different types of boundary conditions is presented here. The comparison was based on the total surface area available for imbibition and corresponding times taken for saturating a core until residual oil saturation. **Fig. 10** shows oil recovery curves for four types of boundary conditions: AFO, TEO, TEC, and OEO. As can be observed from the figure, the

model with OEO type of boundary condition exhibits the smallest oil recovery, while the model with AFO type of boundary condition exhibits the largest value of oil recovery. The former type of boundary condition has only one face of the core available for imbibition, while the latter type of boundary condition has six faces of the core open for imbibition.

Fig. 11 is a plot of absolute time of imbibition as a function of the number of faces available for imbibition. It is observed from Fig. 8 that the time required for saturating a core with water until residual oil saturation increases exponentially, as the number of faces available for imbibition decreases. The comparison of all four types of boundary conditions shows that a non-wetting recovery for the AFO type of model is most efficient and fast, as compared with all other cases.

Effect of Heterogeneity on the Imbibition Oil Recovery. The effect of heterogeneities on oil recovery has received limited treatment in the petroleum literature. The effect of varying permeability profiles along the core on oil recovery was investigated here. It is well known that under the influence of the capillary forces water imbibes from the more permeable zones of porous medium into the less permeable zones and displaces oil. However, without experimental or numerical studies it is difficult to determine oil displacement from the more permeable zone into the less permeable. The same problem could be brought up when water displaces oil from high permeable oil lenses into the less permeable zones of porous medium. For further investigation of the problem, numerical analyses have been performed.

To formulate the problem, a core with only one imbibing face open to fluid flow was considered. The permeability has been varied along the core. Particularly, two cases have been considered: the first case is when oil has been displaced by water and the permeability of the core was decreasing from the bottom to the top of the core; the second case is when permeability was increasing from the bottom to the top. A schematic of both cases is shown in **Fig. 12**. The core on the scheme has been conditionally divided into four parts for allowing a reader to understand the permeability change along the core. For the computational ease the permeability variance along the core was distributed linearly **Fig. 13**. This study was based on the numerical simulation, using the previously matched model of the spontaneous imbibition. The gravity effect was neglected.

The following J-Function was used to scale capillary pressures to account for the differences in block permeability:

$$J(S_w) = \frac{P_c}{s \cos \theta} \sqrt{\frac{k}{f}} \quad (6)$$

The Jfunction has the effect of normalizing all curves to approach a single curve. The results of numerical analyses are shown in **Fig. 14**. From the figure it was observed that oil recovery curves for both cases have generally known shape, but different oil recovery values. From the figure it is clear that capillary displacement of oil by water is more efficient for a case when water imbibes into the core in the direction of decreasing permeability.

The explanation lies in understanding the mechanism of capillary displacement and also realizing that capillary pressure is an inversely proportional function of permeability, which means that when permeability decreasing the capillary pressure is increasing or vice-versa. So when water imbibes in the direction of decreasing permeability, it reaches the boundary of two different permeability zones and without any difficulty moves into the next zone. This unhampered movement occurs because water moves from the zones of low capillary forces into the zones with high capillary forces.

The case is different when the permeability of a porous medium increases in the direction of water imbibition. Water imbibed into the low permeable zone of the core moves ahead under the influence of capillary forces and, finally, reaches the boundary of the high permeable zone. At this point, the further movement of water is getting hindered because water moves into the zone with low capillary forces. So, the analyses indicated that oil displacement from a porous medium, consisting of the sequential zones of different permeabilities, is more efficient, if imbibition occurs in the direction of decreasing permeability than in the direction of increasing permeability.

Parametric Study

This parametric study was based on the numerical simulation, using the previously matched model of the spontaneous imbibition. The gravity effect was neglected. The first series of computer runs were conducted to study the change in imbibition recovery, which was expected with the change in viscosities of the reservoir fluids. The second series considered the changes caused by different capillary pressure and relative permeability curves. The third set of computer runs was conducted to examine oil recoveries for the models with different fracture spacing. Other reservoir and fluid properties were held constant.

Effect of Water-Oil Viscosity Ratio. Fluid viscosity can significantly affect the rate of imbibition. The effect of different water-oil viscosity ratios, at which water imbibed into the core, was examined. The original water-oil ratio used in the base case model was 0.68:3.52. To examine the effect of oil viscosity on imbibition oil recovery, the simulation runs were made for two different oil viscosities: 0.352 and 50 cp. The water viscosity was held constant at 0.68 cp. The first case with 0.68:0.352 water-oil viscosity ratio simulated the case with favorable fluid flow mobility. The second case with 0.68:50 water-oil viscosity ratio simulated the case with unfavorable fluid flow mobility.

The effect of different oil viscosities on the oil recovery for AFO type of spontaneous imbibition model is shown in **Fig. 15**. From the figure it can be observed that the lower the oil viscosity, the bigger the volumes of oil produced from the core as a function of time. As oil viscosity increases, less and less water is imbibed into the core plug. Exactly the same picture has been observed with three other types of imbibition models.

Effect of Capillary Pressure and Relative Permeability. Capillary pressure is a function of pore sizes and the interfacial tension between the fluids in the matrix and the driving force during spontaneous imbibition. In general, the smaller the pore size, or the higher the interfacial tension, the stronger the capillary pressure.

To investigate the sensitivity of imbibition capillary pressure on the imbibition oil recovery, two different capillary pressures were used with the multiplication in order of 0.1 (Case 1) and 10 (Case 2) to the matching results of capillary pressure. These series of simulation runs were made to determine the effect on imbibition of changing capillary pressure. AFO type of the spontaneous imbibition model was used. Other data used in the simulator remained unchanged.

Changes in the imbibition oil recovery for these cases are clearly demonstrated in **Fig. 16**. It can be seen that the change from the Base Case to Case 1 caused a decrease in the oil recovery. Also, the change of capillary pressure from the Base Case to Case 2 caused an increase in spontaneous imbibition oil recovery.

Capillary pressure is assumed to be the only driving force in the spontaneous imbibition process. Thus, increasing the capillary pressure increased the imbibition recovery as shown in Fig 16. Likewise, the decrease of imbibition oil recovery from the Base

Case to Case 1 was also based on the fact that capillary pressure of Case 1 was lower than that of the Base Case.

To investigate the sensitivity of relative permeability curves on the imbibition oil recovery, two cases were run. These two cases represent relative permeabilities as results of multiplication of 0.1 and 0.5 to the matching results of relative permeability. The results in **Figs. 17** and **18** show that oil recovery by imbibition is sensitive to the oil relative permeability curves, while no significant effect was observed in changing the water relative permeability curves. The imbibition oil recovery was sensitive to the oil relative permeability. This can be explained by the fact that a capillary diffusion coefficient is a function of the square of oil relative permeability and, thus, affects the imbibition process much stronger.

Effect of Fracture Spacing. The effect of different fracture spacing was investigated on the Two Ends Open type of model. Fracture spacing is the distance between parallel fracture planes. The top and the bottom of the model, which were open to water imbibition, have been assumed as fracture planes and the distance between the top and the bottom of the model has been varied to study the effect on oil recovery. Different fracture spacing has been obtained by multiplying original fracture spacing by 2, 4, and 8.

Fig. 19 presents a comparative study of time rates of spontaneous imbibition of water for different fracture spacing. The comparison here was based on the fracture spacing and the corresponding times taken to saturate the core until residual oil saturation. As the fracture width increases the time required for saturating a core with water until residual oil saturation increases linearly.

Scaling of Static Imbibition Data

Spontaneous imbibition is an important phenomenon in oil recovery from fractured reservoirs, where the rate of mass transfer between the rock matrix and the fractures determines the oil production. Imbibition is also important in evaluation of wettability of fluid/liquid/porous media system. The rate of imbibition depends primarily on the porous media, the fluids, and their interactions. These include relative permeabilities, matrix shapes, boundary conditions, fluid viscosity, interfacial tension (IFT), and wettability. Laboratory results need to be scaled to estimate oil recovery from the reservoir matrix blocks that have shapes, sizes, and boundary conditions different from those of the laboratory core samples. Upscaling of imbibition oil

recovery from the small reservoir core sample allows us to predict field performance.

The basic requirements for scaling laboratory data to field conditions were investigated by Rapoport.⁴ In scaling imbibition results for different oil/brine/rock systems or in predicting field performance from laboratory measurements, Mattax and Kyte⁵ proposed the following scaling group:

$$t_D = t \sqrt{\frac{k_m}{f}} \frac{s}{m_w} \frac{1}{L^2} \quad (7)$$

where t_D is dimensionless time, t is imbibition time, k_m is matrix permeability, f is porosity, s is IFT, μ_w is water viscosity, and L is core length. The assumptions made in deriving this equation were that the sample shapes must be identical, the oil/water viscosity ratio must be duplicated, the gravity effects must be neglected, initial fluid distribution must be duplicated, the capillary pressure functions must be related by direct proportionality, and the relative permeability functions must be the same.

In oil production from fractured reservoirs, the systems with different matrix sizes, shapes, and boundary conditions will give different mass transfer rates between the fractures and the rock matrix. The smaller the ratio of a volume to open surface area, the faster the imbibition rate. So, based on the work of Mattax and Kyte⁵ and Kazemi *et al.*⁶ a characteristic length was proposed by Ma *et al.*,⁷ which was defined as follows:

$$L_C = \sqrt{\frac{V}{\sum_{i=1}^n \frac{A_i}{x_{Ai}}}} \quad (8)$$

where V is the bulk volume of the matrix, A_i is the area open to the imbibition at the i th direction and x_{Ai} is the length defined by the shape and boundary conditions of the matrix block. Because one of the assumptions in deriving Eq. 7 is that viscosity ratios are identical, Ma *et al.*⁷ also proposed to use oil viscosity in Eq. 7, provided that the viscosity ratio is constant, taking into consideration from the recent studies that for water/oil systems imbibition rate is proportional to the geometric mean of the water and oil phase viscosities:

$$m_s = \sqrt{m_o m_w} \quad (9)$$

So, to account for both the effect of viscosity ratio and boundary conditions, the following modified scaling group was proposed by Ma *et al.*:⁷

$$t_D = t \sqrt{\frac{k_m}{f}} \frac{s}{m_s} \frac{1}{L_C^2} \quad (10)$$

Scaling for Different Types of Boundary Conditions.

In the present work, the applicability of Eq. 10 was tested through extensive numerical study of the effect of boundary conditions. Two types of boundary conditions have been examined: One End Open and Two Ends Open. Then the results from numerical studies of spontaneous imbibition mechanism were used to compare between Eq. 7 and Eq. 10. The comparison has been performed on the semi-log plot of oil recovery vs. dimensionless time.

Fig. 20 shows correlation of results for different boundary conditions using Eq. 7. **Fig. 21** shows correlation of results for different boundary conditions using characteristic length in Eq. 10. Comparison of both figures revealed the fact that points are more scattered in Fig. 20 than in Fig. 21. This fact proved that using characteristic length in the equation of dimensionless time improves the correlation for the models with different boundary conditions.

Scaling for Variable Mobility Ratios. Here, the new scaling group proposed to correlate simulation results has been compared to the early upscaling technique. The previous scaling studies of spontaneous imbibition was not focused the varying mobilities of the fluids. Therefore, it was decided to study this effect and compare results from the previous upscaling technique (Eq. 10) to the results from the newly developed scaling equation.

The newly developed scaling technique has been proposed by Zhou *et al.*⁸ They included characteristic mobilities of a wetting and a non-wetting phase into the equation of dimensionless time. The equation is as follows:

$$t_D = t \sqrt{\frac{k_m}{f}} \frac{s}{L_C^2} \sqrt{I_w I_{NW}} \frac{1}{\sqrt{M+1} \sqrt{M}} \quad (11)$$

where

$$I = \frac{k}{m} \quad (12)$$

and

$$M = \frac{I_w}{I_{NW}} \quad (13)$$

The parameter λ is a characteristic mobility for a wetting and a non-wetting phase, and M is characteristic mobility ratio. Here, end-point relative permeabilities are used when calculating λ and M . The mobility ratios also depend on the viscosity of fluids. The above equation is valid, only if relative permeability and capillary pressure functions are similar for all of the measurements. **Figs. 22 and 23** show comparison between the newly proposed upscaling method (Eq. 11) and previous upscaling technique (Eq. 10). The comparison is shown for two types of boundary conditions: Two Ends Open, and One End Open.

Three mobility ratios have been considered. The first case was with favorable mobility ratio, the second case was with unit mobility ratio, and the third case was with unfavorable mobility ratio. In all cases, oil viscosity has been altered, and water viscosity remained unchanged. From both figures it could be observed that the curves fall into a narrow range, when we use the newly developed scaling technique. The scaling is almost perfect with slight differences at late times. These differences, probably, result from the influence of the boundary of the porous medium on imbibition. When using a previous scaling equation, the data is more scattered.

We observed a very good correlation for the results of spontaneous imbibition with the new scaling technique. The recovery curves agree reasonably well for all mobility ratios. The data are reduced to a single curve in spite of the fact that nonwetting fluid viscosity varies by 3 orders of magnitude. The results indicate that the new dimensionless time can significantly improve the scaling of spontaneous imbibition.

Conclusions

The following conclusions have been derived from this study:

1. The comparative study of time rates of water spontaneous imbibition for different types of boundary conditions revealed the fact that the time required for capillary imbibition until residual oil saturation increases exponentially, as the number of faces available for imbibition decreases.
2. The comparison of all four types of boundary conditions showed that oil recovery for the All Faces Open type of a model is most efficient and fast, as compared with all other cases.

3. The effect of varying permeability profiles along the core on oil recovery showed that when water imbibes in the direction of decreasing permeability, oil recovery is higher than when water imbibes in the direction of increasing permeability.
4. The study of the effect of different water-oil viscosity ratios, at which water imbibed into the core, showed that the lower the oil viscosity, the greater the volumes of oil produced from the core as a function of time.
5. The results showed that increasing the capillary pressure increased imbibition recovery. Oil recovery by imbibition was sensitive to oil relative permeability curves, while no significant effect was observed in changing the water relative permeability curves.
6. A comparative study of time rates of spontaneous imbibition of water for different fracture spacing showed that the time required for capillary imbibition until residual oil saturation increased linearly, as the fracture space increased.
7. The characteristic length described by Ma *et al'* in the equation of dimensionless time improved a correlation between data points for the models with different boundary conditions.
8. The spontaneous imbibition results of this study have been upscaled to the field dimensions. The validity of a new definition of characteristic length used in the modified scaling group has been evaluated. The new scaling group used to correlate simulation results has been compared to the early upscaling techniques.
9. The new technique used for upscaling, significantly improved correlations by taking end-point fluid phase mobilities and the mobility ratios into account. The comparison between the new and the previous dimensionless times proved that even if non-wetting fluid viscosity varies by 3 orders of magnitude, the data could be reduced to a single curve, if we use new dimensionless time definition.

Nomenclature

A	= Total area, ft ²
B_o	= Bond Number
D	= Diameter, ft
g	= Gravitational acceleration, ft/sec ²
H	= Height, ft
$J(S_w)$	= Leverett J-function

k	= Permeability, md
k_{ro}	= Oil relative permeability
k_{rw}	= Water relative permeability
L	= Length, ft
L_c	= Characteristic length, ft
M	= Mobility ratio
P_c	= Capillary pressure, psi
P_{nw}	= Pressure of non-wetting phase, psi
P_w	= Pressure of wetting phase, psi
r	= Pore radius, ft
R	= Oil recovery, %
R_g	= Ultimate recovery, %
R_{imb}	= Imbibition oil recovery, %
S_w	= Water saturation, fraction
S_{wi}	= Irreducible water saturation, fraction
S_{nwr}	= Residual saturation, fraction
S_e	= Effective water saturation, fraction
t	= Time, min
t_d	= Dimensionless time
t_c	= Dimensionless time for high capillary gravity ratio
t_g	= Dimensionless time for low capillary gravity ratio
V	= Volume, ft ³
μ_o	= Oil viscosity, cp
μ_w	= Water viscosity, cp
μ_g	= Geometric mean of the water and oil phase viscosities, cp
ρ	= Density, ft/lb ³
ϕ	= Porosity, fraction
σ	= Interfacial tension, dynes/cm
θ	= Contact angle, degrees
λ	= Phase mobility, md/cp

References

1. Brownscombe, E.R., and Dyes, A.B.: **Water-Imbibition Displacement... Can it Release Reluctant Spraberry Oil?** *Oil and Gas J.* (17 November 1952) 264-265.
2. Kleppe, J., and Morse, R.A.: **Oil Production from Fractured Reservoirs by Water Displacement** Paper SPE 5084 presented at the *SPE-AIME 49th Annual Fall Meeting*, Houston, Texas, 6-9 October.
3. Putra, E., Fidra, Y. and Schechter, D.S.: **Study of Waterflooding Process in Naturally Fractured Reservoirs from Static and Dynamic Imbibition Experiments.** Paper SCA 9910 presented at the *1999 International Symposium of the Society of Core Analysts* Colorado, Aug. 1-4.
4. Rapoport, L.A.: **Scaling Laws for Use in Design and Operation of Water/Oil Flow Models.** In *Trans., AIME* (1955) 204, 143.
5. Mattax, C.C., and Kyte, J.R.: **Imbibition Oil Recovery from Fractured, Water-Drive Reservoirs.** *SPEJ* (June 1962) 177-184; In *Trans., AIME*, 225.
6. Kazemi, H., Gilman, J.R., and Elsharkawy, A.M.: **Analytical and Numerical Solution of Oil Recovery from Fractured Reservoirs with Empirical Transfer Functions.** Paper SPE 6192 presented at the *1976 SPE Annual Technical Conference and Exhibition*, New-Orleans, Louisiana, 3-6 October.
7. Ma, S., Zhang, X., and Morrow, N.R.: **Experimental Verification of a Modified Scaling Group for Spontaneous Imbibition.** Paper SPE 30762 presented at the *1995 SPE Annual Technical Conference and Exhibition*, Dallas, Texas, 22-25 October.
8. Zhou, D., Jia, L., Kamath, J., and Kovscek, A.R.: **An Investigation of Counter-Current Imbibition Process in Diatomite.** Paper SPE 68837 presented at the *2001 SPE Western Regional Meeting*, Bakersfield, California, 26-30 March.

Table 1 – Physical Properties of the Core and Brine

Property	Value	Unit
Dimensions of the core	3.2 x 3.2 x 4.9	cm
Porosity	15.91	%
Permeability	74.7	md
Initial water saturation	41.61	%
Viscosity of oil	3.52	cp
Density of oil	0.8635	g/cm ³
API	31	°
Viscosity of water	0.68	cp
Density of water	1	g/cm ³

0.6113	0.09	0.0288	0.651
0.6290	0.1071	0.0148	0.547
0.6468	0.1257	0.0062	0.345
0.6645	0.1458	0.00018	0.254
0.6823	0.1674	0.00015	0.134
0.7	0.2	0	0

Table 2 – Table of Grid Sizes Investigated in the Grid Sensitivity Analyses

Number of Simulation Run	No. of gridblocks in I, J and K directions			Total number of gridblocks
	I-Direction	J-Direction	K-Direction	
1	7	7	7	343
2	12	12	12	1,728
3	16	16	16	4,096
4	20	20	20	8,000
5	20	20	25	10,000

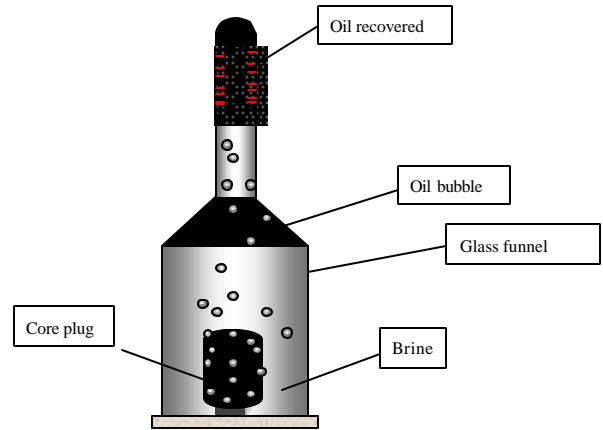


Fig. 1 – Spontaneous Imbibition Cell³

Table 3 – Properties of the Core for Numerical Simulation

Property	Value	Unit
Number of grid blocks in X -Direction	20	-
Number of grid blocks in Y -Direction	20	-
Number of grid blocks in Z-Direction	20	-
Grid block dimension X-Direction	0.178	cm
Grid block dimension Y-Direction	0.178	cm
Grid block dimension Z-Direction	0.242	cm
Density of oil	0.8635	g/cm ³
Density of water	1	g/cm ³
Viscosity of oil	3.52	cp
Viscosity of water	0.68	cp
Permeability	74.7	md
Porosity	0.1591	-
Initial water saturation	(2-19x2-19x2-19)*0.4161	-
Boundary condition	All sides	-

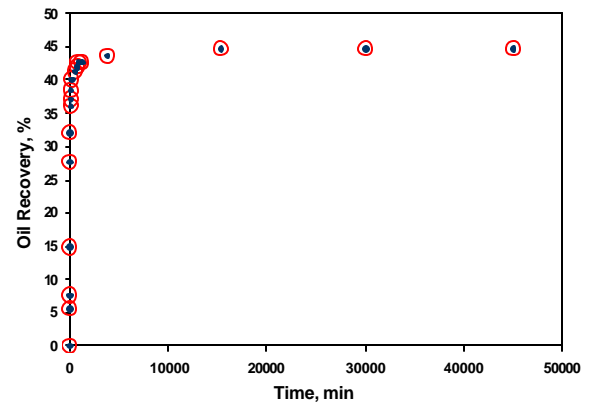


Fig. 2 – Oil recovery curve from static imbibition experiment.

Table 4 – Table of Relative Permeabilities and Capillary Pressure

Water Saturation, Fraction	Water Relative Permeability	Oil Relative Permeability	Capillary Pressure, Psi
0.4161	0	0.9	1.7537
0.4338	0.0007	0.7787	1.555
0.4516	0.003	0.6331	1.445
0.4693	0.0067	0.5069	1.375
0.4871	0.0119	0.3967	1.273
0.5048	0.0186	0.3071	1.164
0.5226	0.0268	0.2307	1.078
0.5403	0.0365	0.1682	0.976
0.5581	0.0476	0.1181	0.922
0.5758	0.0603	0.0791	0.828
0.5935	0.0744	0.0498	0.733

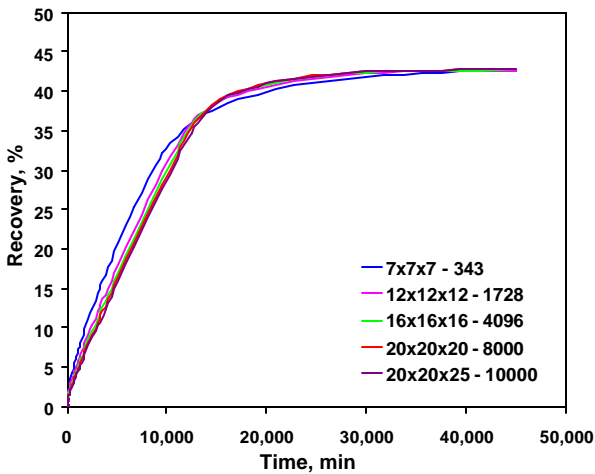


Fig. 3 – Grid size effect on oil recovery from static imbibition experiment.

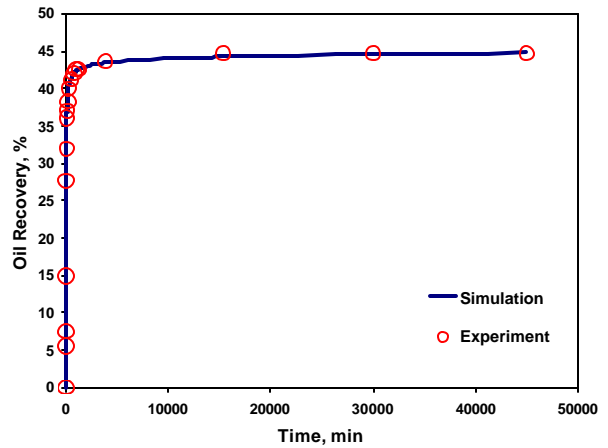


Fig. 6 – Match of the simulated oil recovery with the observed oil recovery.

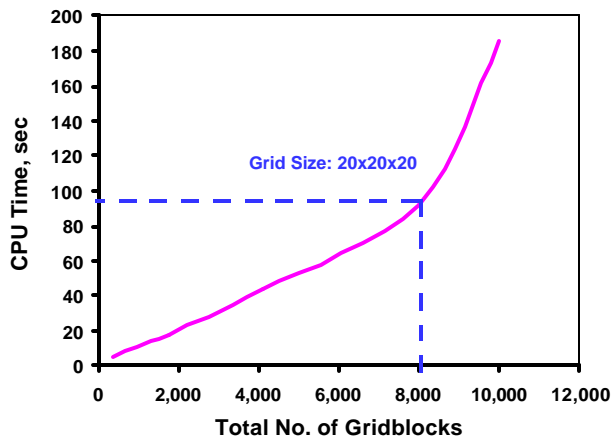


Fig. 4 – Simulation times for different grid sizes.

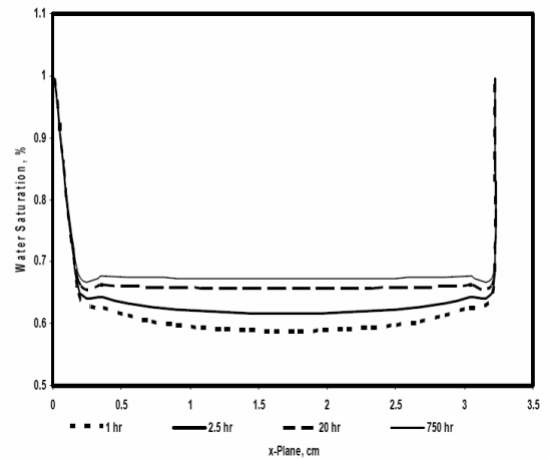


Fig. 7 – Water distribution at different imbibition times from x-plane view.

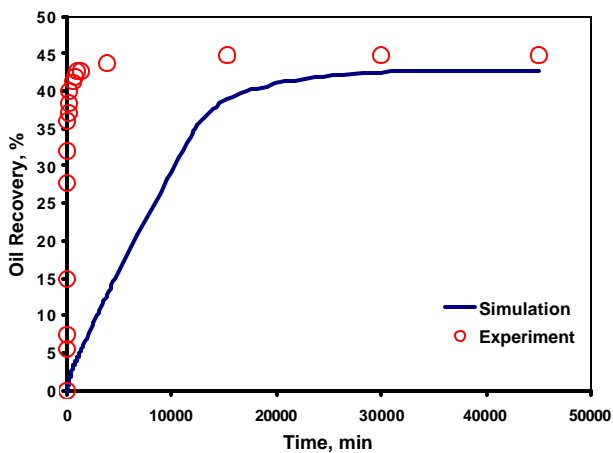


Fig. 5 – Observed oil recovery vs. simulated before adjustment of reservoir data.

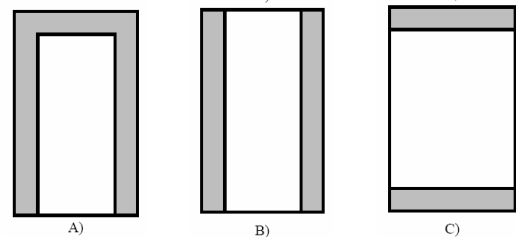


Fig. 8 – Schematic representation of imbibition in cores with different boundary conditions: A) One End Open, B) Two Ends Open, and C) Two Ends Closed types.

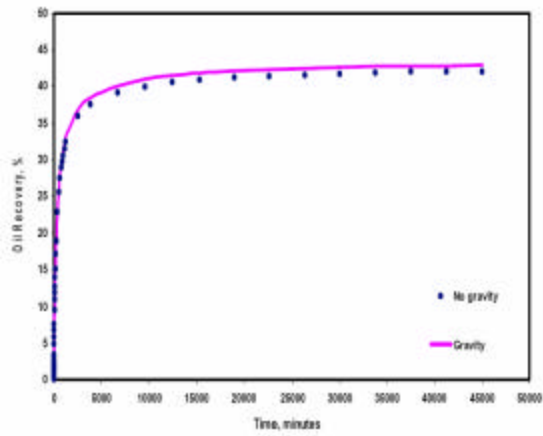


Fig. 9 – Effect of gravity on imbibition response.



Fig. 12 – OEO imbibition model: first case $k_1 > k_2 > k_3 > k_4$ and second case $k_1 < k_2 < k_3 < k_4$.

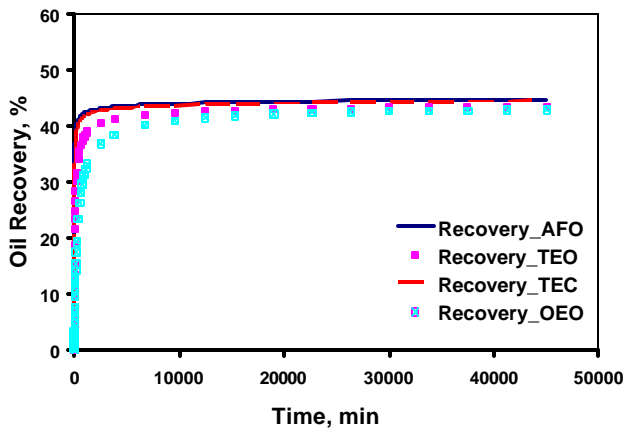


Fig. 10 – Oil recoveries for All Faces Open, Two Ends Closed, Two Ends Open, and One End Open types of boundary conditions.

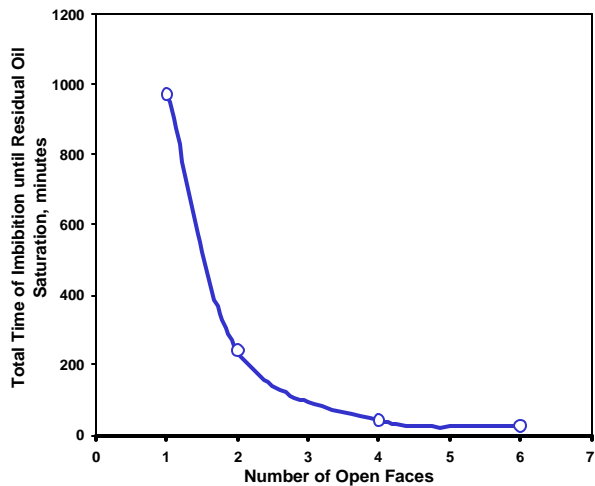


Fig. 11 – Absolute time for imbibition to reach S_{or} as a function of the faces available for imbibition.

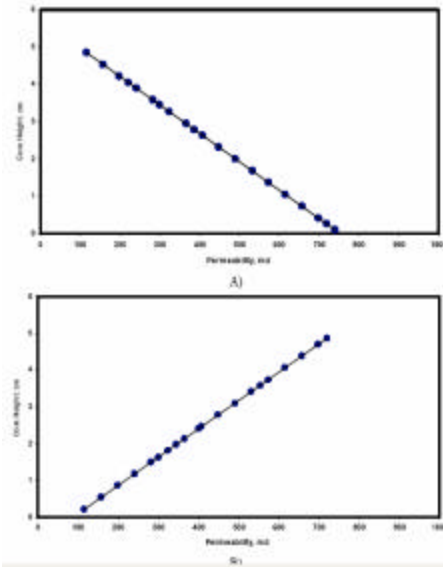


Fig. 13 – Permeability profiles along the core: A) $k_1 > k_2 > k_3 > k_4$, B) $k_1 < k_2 < k_3 < k_4$.

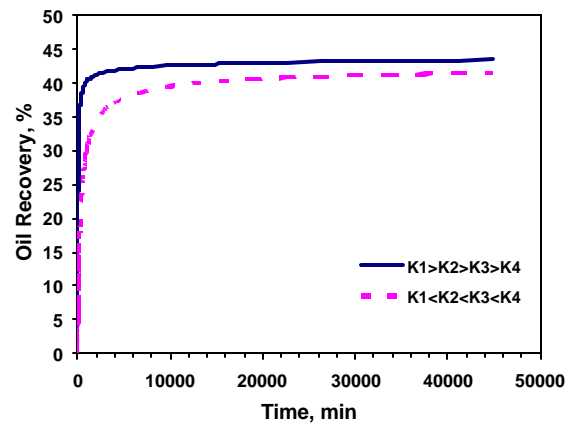


Fig. 14 – Oil recovery curves for different permeability profiles along the core.

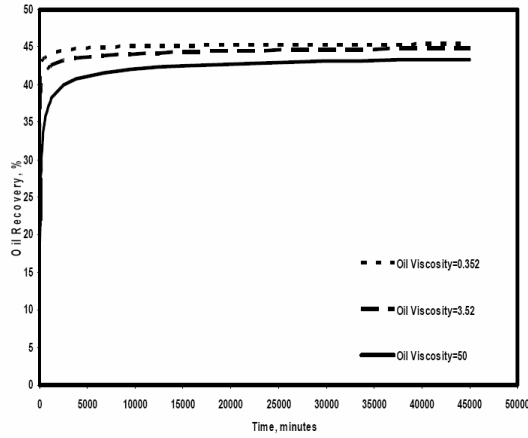


Fig. 15 – Oil recovery curves with different oil viscosities.

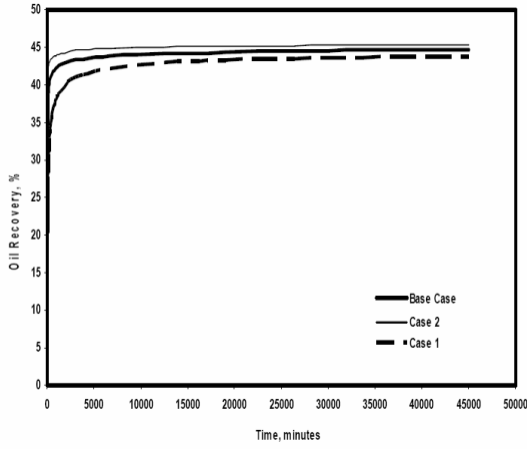


Fig. 16 – Effect of different capillary pressure on oil recovery.

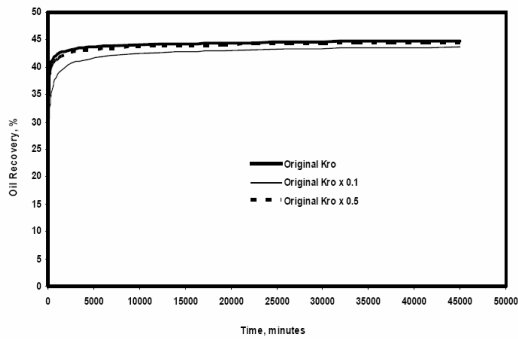


Fig. 17 – Effect of different oil relative permeabilities on oil recovery.

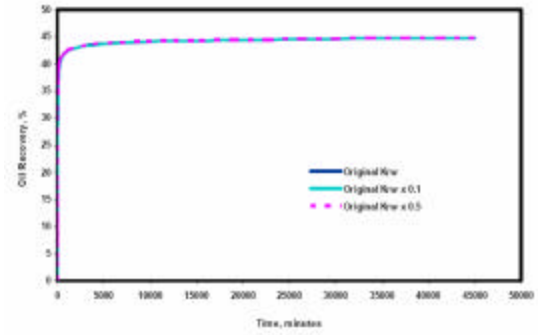


Fig. 18 – Effect of different water relative permeabilities on oil recovery.

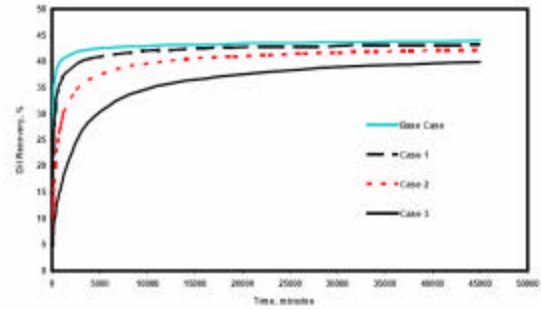


Fig. 19 – Effect of different fracture spacing on oil recovery.

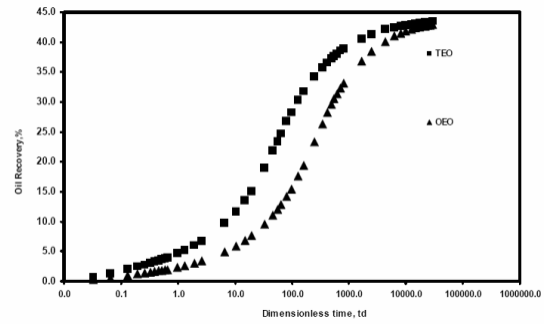


Fig. 20 – Correlation of the results for the systems with different boundary conditions, using the length of the core in the equation of dimensionless time.

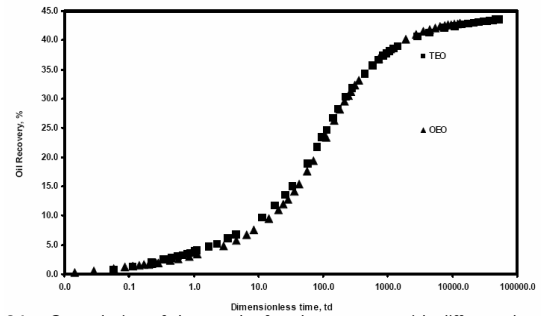


Fig. 21 – Correlation of the results for the systems with different boundary conditions, using the characteristic length in the equation of dimensionless time.

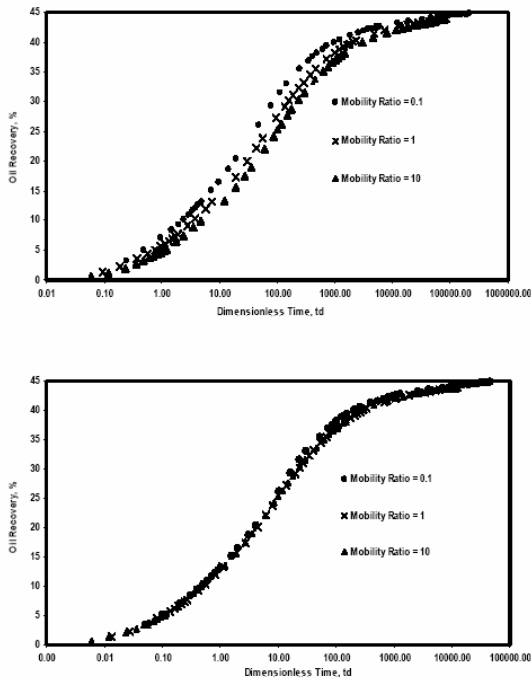


Fig. 22 – Comparing correlation of the results for the systems with different mobility ratios using Eq. 10 and Eq. 11 – Two Ends Open.

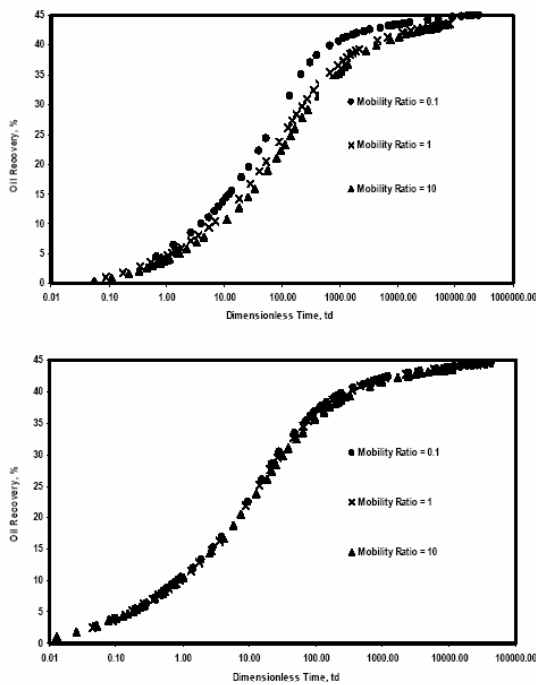


Fig. 23 – Comparing correlation of the results for the systems with different mobility ratios using Eq. 10 and Eq. 11 – One End Open.